AMERICAN SOCIETY FOR MICROBIOLOGY | Journal of Virology®

VIRUS-CELL INTERACTIONS

Filamentous Structures Induced by a Phytoreovirus Mediate Viral Release from Salivary Glands in Its Insect Vector

Qianzhuo Mao, Zhenfeng Liao, Jiajia Li, Yuyan Liu, Wei Wu, Hongyan Chen, Qian Chen, Dongsheng Jia, Taiyun Wei

Fujian Province Key Laboratory of Plant Virology, Institute of Plant Virology, Fujian Agriculture and Forestry University, Fuzhou, Fujian, People's Republic of China

ABSTRACT Numerous viral pathogens are persistently transmitted by insect vectors and cause agricultural or health problems. These viruses circulate in the vector body, enter the salivary gland, and then are released into the apical plasmalemma-lined cavities, where saliva is stored. The cavity plasmalemma of vector salivary glands thus represents the last membrane barrier for viral transmission. Here, we report a novel mechanism used by a persistent virus to overcome this essential barrier. We observed that the infection by rice gall dwarf virus (RGDV), a species of the genus *Phytoreovirus* in the family *Reoviridae*, induced the formation of virus-associated filaments constructed by viral nonstructural protein Pns11 within the salivary glands of its leafhopper vector, *Recilia dorsalis*. Such filaments attached to actin-based apical plasmalemma and induced an exocytosis-like process for viral release into vector salivary gland cavities, through a direct interaction of Pns11 of RGDV and actin of *R. dorsalis*. Failure of virus-induced filaments assembly by RNA interference with synthesized double-stranded RNA targeting the Pns11 gene inhibited the dissemination of RGDV into salivary cavities, preventing viral transmission by *R. dorsalis*. For the first time, we show that a virus can exploit virus-induced inclusion as a vehicle to pass through the apical plasmalemma into vector salivary gland cavities, thus overcoming the last membrane barrier for viral transmission by insect vectors.

IMPORTANCE Understanding how persistent viruses overcome multiple tissue and membrane barriers within the insect vectors until final transmission is the key for viral disease control. The apical plasmalemma of the cavities where saliva is stored in the salivary glands is the last barrier for viral transmission by insect vectors; however, the mechanism is still poorly understood. Here we show that a virus has evolved to exploit virus-induced filaments to perform an exocytosis-like process that enables viral passage through the apical plasmalemma into salivary cavities. This mechanism could be extensively exploited by other persistent viruses to overcome salivary gland release barriers in insect vectors, opening new perspectives for viral control.

KEYWORDS plant reovirus, RGDV, insect vector, salivary gland barrier, Pns11 filament, viral transmission

Received 15 February 2017 **Accepted** 30 March 2017

Accepted manuscript posted online 5 April 2017

Citation Mao Q, Liao Z, Li J, Liu Y, Wu W, Chen H, Chen Q, Jia D, Wei T. 2017. Filamentous structures induced by a phytoreovirus mediate viral release from salivary glands in its insect vector. J Virol 91:e00265-17. https://doi.org/10.1128/JVI.00265-17.

Editor Anne E. Simon, University of Maryland, College Park

Copyright © 2017 American Society for Microbiology. All Rights Reserved.

Address correspondence to Taiyun Wei, weitaiyun@fafu.edu.cn.

Numerous viral pathogens that cause significant global agricultural as well as health problems are persistently transmitted by insect vectors, such as mosquitoes, planthoppers, aphids, leafhoppers, thrips, and whiteflies (1–4). Such vector-borne viruses establish their initial infection in the insect midgut and disseminate to the hemolymph and finally into the salivary glands, from where they are introduced into susceptible hosts (1–4). Thus, elucidating how viruses overcome multiple tissue and membrane barriers in insect bodies is important for controlling these viral diseases.

Persistent viruses are classified into two groups: propagative and nonpropagative viruses (1). All arthropod-borne animal viruses (arboviruses) and persistent propagative plant viruses can replicate and induce viral inclusions in their respective insect vectors (1). The midgut and salivary gland are the two major barriers for viral transmission by insect vectors (1, 2). Electron microscopy revealed that persistent nonpropagative luteoviruses overcome midgut barriers by intact virions (5, 6). In contrast, viral inclusions of persistent propagative viruses can facilitate viral spread in the midgut of insect vectors (1, 2, 7). For example, rice dwarf virus (RDV), a phytoreovirus in the family *Reoviridae*, exploits the tubules constituted by viral nonstructural protein Pns10 to pass through the microvilli of midgut epithelium into the lumen of the leafhopper vector (7, 8). Southern rice black streaked dwarf virus (SRBSDV), a fijivirus in the family *Reoviridae*, exploits the tubules constituted by viral nonstructural protein P7-1 to pass through the basal lamina from the midgut epithelium into the visceral circular muscle of the white-backed planthopper vector (7, 9). Furthermore, we have shown that a tenuivirus, rice stripe virus, exploits the filamentous or amorphous inclusions constructed by the nonstructural protein NS4 to facilitate the efficient spread of viral ribonucleoprotein in the midgut epithelium of the small brown planthopper (10). Although studies have begun to understand the mechanisms for overcoming the midgut barriers, the mechanisms used by persistent viruses to overcome the salivary gland barriers are still poorly understood.

Insect salivary gland cells are filled with abundant apical plasmalemma-lined cavities, where saliva is stored. Generally, virions are secreted together with saliva to the salivary cavities and then to the canal in the stylet, to be ejected while insect vectors feed on susceptible hosts (1, 4). Previous studies have focused on the routes for viral spread into the salivary glands of insect vectors (1, 4, 7, 11). To be transmitted, persistent viruses must pass through the cavity apical plasmalemma of salivary gland cells, and thus, such plasmalemma represents the last membrane barrier for viral transmission by insect vectors (1, 2, 4, 12). The use of secretory cells in the central region of principal salivary glands (PSGs) of the whitefly *Bemisia tabaci* has been approved to determine the recognition and transmission of begomoviruses (13). Thus, the ability for a virus to pass through the apical plasmalemma of salivary cavities is a major determinant of vector competence for a virus (1, 4, 7). However, the mechanism(s) used by viruses for overcoming this membrane barrier is poorly documented. It is generally known that nonpropagative luteoviruses and propagative rhabdoviruses can overcome this barrier via transcytosis or membrane budding, as revealed by electron microscopy (2, 6). The natural mechanisms used by persistent viruses to overcome cavity plasmalemma barriers of salivary glands in insect vectors are unknown.

In this study, we used rice gall dwarf virus (RGDV), a phytoreovirus in the family *Reoviridae*, and its main vector, leafhopper *Recilia dorsalis*, to reveal how a propagative virus overcomes the plasmalemma barriers of insect salivary glands. RGDV was first described in 1979 in Thailand and causes severe epidemics in southern China and Southeast Asia (14, 15). RGDV is transmitted, with high efficiency and in a persistent-propagative manner, mainly by *R. dorsalis* (15). RGDV has icosahedral and double-shelled particles approximately 65 to 70 nm in diameter (16). The viral genome consists of 12 segments (S1 through S12) of double-stranded RNAs (dsRNAs) (17, 18). The segments S1, S2, S3, S5, S6, and S8 encode the corresponding structural proteins P1, P2, P3, P5, P6, and P8, respectively; the remaining segments of the RGDV genome encode nonstructural proteins (Pns4, Pns7, Pns9, Pns10, Pns11, and Pns12) (17, 18). After ingestion of viral particles by the leafhopper, RGDV first enters the epithelial cells of the filter chamber, where viroplasms composed of nonstructural proteins Pns7, Pns9, and Pns12 are formed for viral replication and assembly of progeny virions (15, 19, 20). Subsequently, RGDV directly crosses the basal lamina into the visceral muscles, from where it spreads into the hemocoel (15). Finally, RGDV invades and replicates in the PSGs (15). During viral infection of a continuous cell line derived from *R. dorsalis*, virus-containing tubules constructed by the nonstructural protein

Pns11 of RGDV, which is orthologous to the nonstructural protein Pns10 of RDV, facilitate viral spread among insect vector cells, but the functional role of Pns11 in the intact insect vector is unclear (21). In this study, we demonstrate that Pns11 of RGDV can form virus-associated filaments in vector PSGs. Most importantly, we found that RGDV can exploit virus-associated Pns11 filaments to perform an exocytosis-like process for viral dissemination via the apical plasmalemma into salivary cavities of its insect vectors.

RESULTS

Dissemination of RGDV into the cavity of vector salivary glands used an exocytosis-like mechanism. The salivary glands of leafhopper consist of two paired sets of principal and accessory glands (22). The PSG functions as the saliva excretory organ and consists of six types of secretory cells termed numerically from I-cells (I) to VI-cells (VI) (Fig. 1A) (22). The salivary gland cells of *R. dorsalis* are filled with apical plasmalemma-lined cavities (Fig. 1B to D). Here, we first used electron microscopy to observe the association of RGDV with the apical plasmalemma of PSG cavities in the viruliferous *R. dorsalis*. In the cytoplasm of secretory cells, RGDV particles were closely associated with one edge of filamentous structures (Fig. 1E). We observed that the virus-free edges of such filaments can attach to the surface of apical plasmalemma (Fig. 1E and F). The attachment of virus-associated filaments with the cavity plasmalemma may have induced membrane curvature (Fig. 1F and G). This curvature change was followed by the formation of different shapes of invaginations at the surface (Fig. 1F and G), which finally created spherical or ellipsoid vesicular structures in the cavities (Fig. 1G and H). RGDV particles were directly accumulated along the inner edges of these invaginations or vesicular compartments (Fig. 1G and H). It was clear that the edges of such invaginations or vesicular compartments were derived from virus-associated filaments in the cytoplasm (Fig. 1I and J). We found that more than 80% of cavities contained virus-associated vesicular compartments in virus-infected PSG regions after testing 50 viruliferous individuals of *R. dorsalis*. Together, our observations suggested that RGDV may use the filaments to perform an exocytosis-like mechanism for virion entry into the cavities by passing through the apical plasmalemma.

Association of nonstructural protein Pns11 of RGDV with actin-based apical plasmalemma mediated viral dissemination into the cavities of vector salivary glands. RGDV infection of insect salivary glands has been shown to induce the formation of various inclusions composed of nonstructural proteins for viral replication or spread (15, 19, 23, 24). We used immunoelectron microscopy to investigate which viral nonstructural proteins (among Pns4, Pns7, Pns9, Pns10, Pns11, and Pns12) were involved in the formation of virus-associated filaments along the apical plasmalemma of PSG cavities in viruliferous *R. dorsalis*. Immunoelectron microscopy showed that Pns11-specific IgG specifically recognized virus-associated filaments in the cytoplasm of secretory cells (Fig. 2A to D), the edges of invaginations along the cavity plasmalemma (Fig. 2E to G), or the surfaces of vesicular compartments in the cavities (Fig. 2H to K). Usually, virus-containing tubules composed of Pns11 were closely associated with the midgut microvilli or muscle fibers of viruliferous *R. dorsalis* (Fig. 2L to N), but they never were observed in the salivary glands. Interestingly, Pns11-specific filaments were not observed in vector midguts. Thus, nonstructural protein Pns11 of RGDV may induce the formation of different viral inclusions in the midguts or salivary glands to perform various functions.

We then used immunofluorescence microscopy to investigate the relationship between Pns11 and actin-based cavity plasmalemma by immunolabeling virus-infected PSGs of *R. dorsalis* with Pns11-fluorescein isothiocyanate (Pns11-FITC) and actin dye phalloidin-rhodamine. Our observations indicated that actin-based cavity plasmalemma formed a loose network to occupy the intracellular space of secretory cells (Fig. 3A and B). In virus-infected PSGs regions, Pns11-specific inclusions were closely associated with the whole actin-based cavity plasmalemma (Fig. 3B to D).

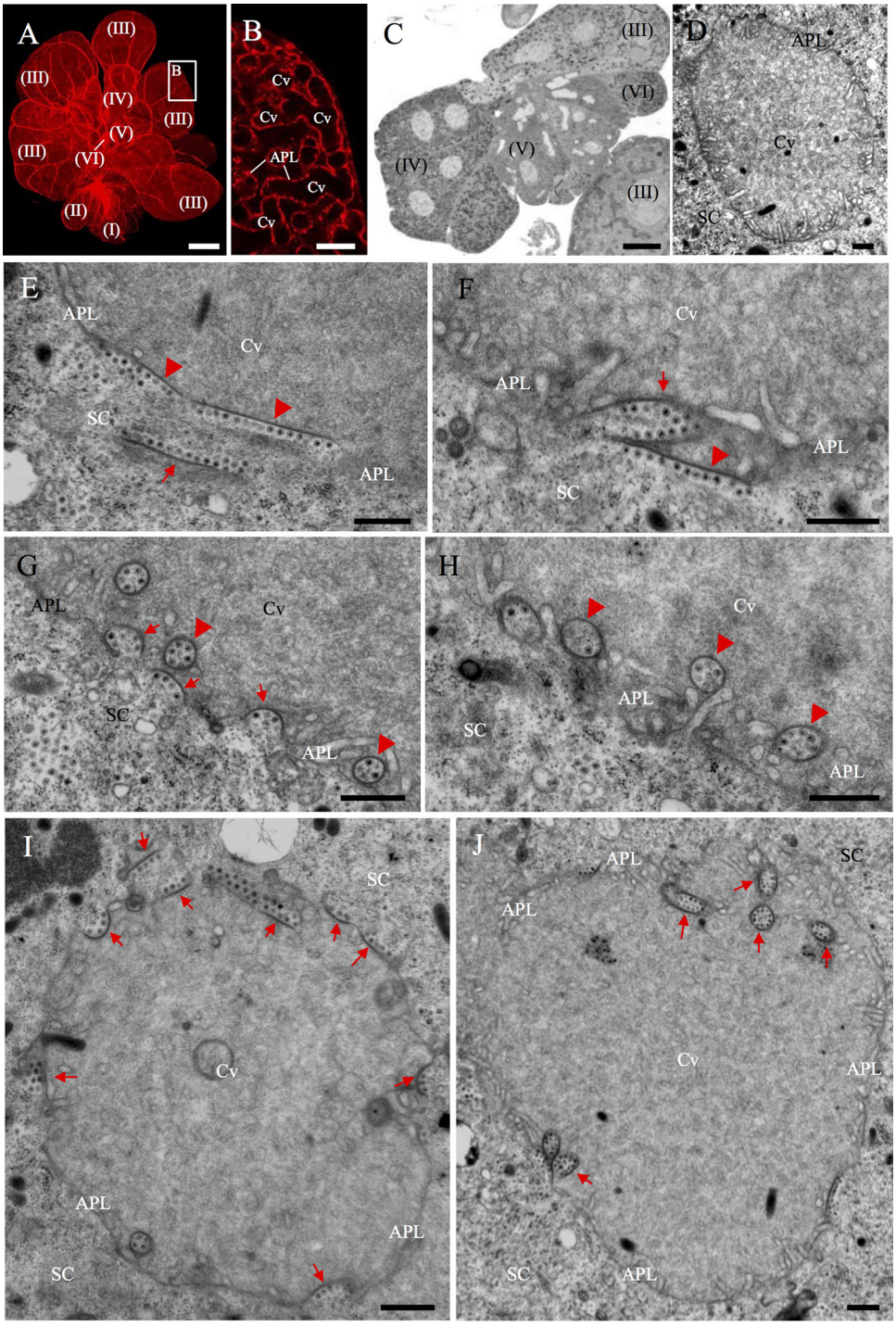

FIG 1 Electron microscopy showing dissemination of RGDV into the apical plasmalemma-lined cavities in the PSGs of *R. dorsalis*. (A) View of dissected PSG of *R. dorsalis*, which was stained for actin with phalloidin-rhodamine (red) and then examined via confocal microscopy. The PSG contained six types of secretory cells termed numerically from I-cells (I) to VI-cells (VI). Bar, 100 μm. (B) Enlarged image of the boxed area in panel A, showing the apical plasmalemma-lined cavities forming a loose network within the III-cell. Bar, 10 μm. (C) Semithin section of PSG, showing the cytological characteristics of several types of cells. Bar, 25 μm. (D) Transmission electron micrograph showing the salivary cavity in III-cells. Bar, 500 nm. (E to H) Transmission electron micrographs showing the dissemination of RGDV particles from the cytoplasm of PSG cells to the salivary cavities. RGDV particles first were associated with one edge of filament (arrow) in cell cytoplasm (E). Such virus-associated filaments were attached to the surface of apical plasmalemma (arrowheads; E and F), which induced the formation of invaginations along the apical plasmalemma (arrows; F and G), and finally the formation of vesicular compartments in the cavity (arrowheads; G and H). (I, J) Two virus-associated salivary cavities, showing the presence of virus-associated inclusions (arrows) in the cytoplasm, along the apical plasmalemma, or in the cavity. Bars, 500 nm. APL, apical plasmalemma; Cv, cavity; SC, salivary cytoplasm.

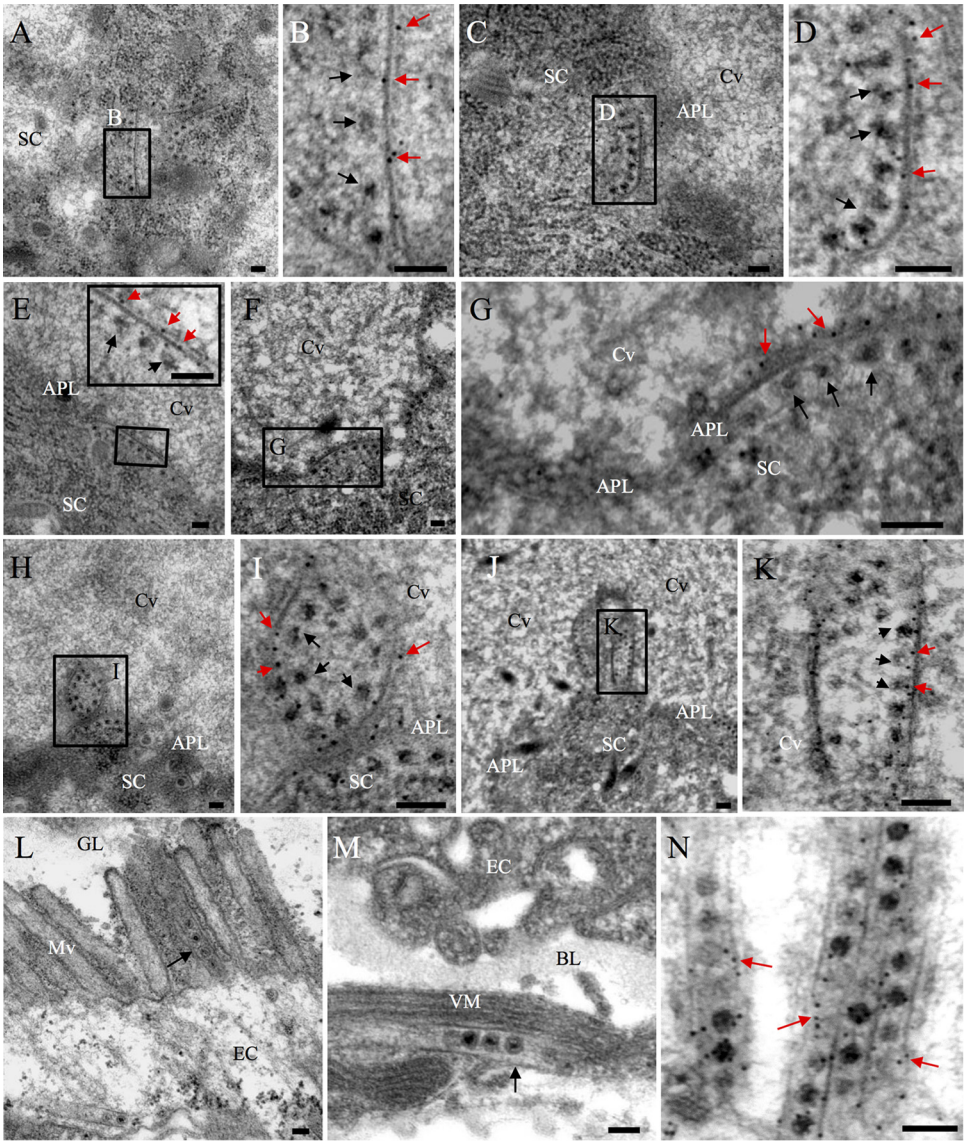

FIG 2 Immunoelectron microscopy showing the distribution of Pns11 of RGDV during viral infection in the PSGs or midguts of *R. dorsalis*. (A to K) Immunogold labeling of Pns11 with virus-associated filaments in the cell cytoplasm (A to D), the edges of invaginations along the apical plasmalemma (E to G), or the surface of vesicular compartments in the cavity (H to K). Virus-infected PSGs were immunolabeled with Pns11-specific IgG as primary antibodies, followed by treatment with 10-nm gold particle-conjugated goat antibodies against rabbit IgG as secondary antibodies. Panels B, D, G, I, and K are enlargements of the boxed areas in panels A, C, F, H, and I, respectively. The inset in panel E is an enlarged image of the boxed area in the same panel. Black arrows mark viral particles, while red arrows mark gold particles. (L, M) Association of virus-containing tubules (black arrows) with midgut microvilli (L) or visceral muscles (M). (N) Immunogold labeling of Pns11 with virus-containing tubules in the midgut epithelium. Red arrows mark gold particles. APL, apical plasmalemma; Cv, cavity; SC, salivary cytoplasm; EC, epithelial cells; GL, gut lumen; BL, basal lamina; VM, visceral muscle. Bars, 100 nm.

Immunoelectron microscopy confirmed that actin was associated with the edges of virus-associated invaginations along the apical plasmalemma (Fig. 3E and F). All these results indicated that virus-associated filaments composed of Pns11 of RGDV had the inherent ability to associate with actin-based cavity plasmalemma in its insect vectors.

To examine how viral particles disseminated into the cavities, PSGs of viruliferous *R. dorsalis* at different days post-first access to diseased plants (padp) were immunolabeled with Pns11-FITC and virus-rhodamine and then processed for immunofluorescence microscopy. At 8 days padp, RGDV had spread from the hemocoel into the PSGs of its insect vectors (Fig. 3G). At 9 days padp, we observed that Pns11 filaments were

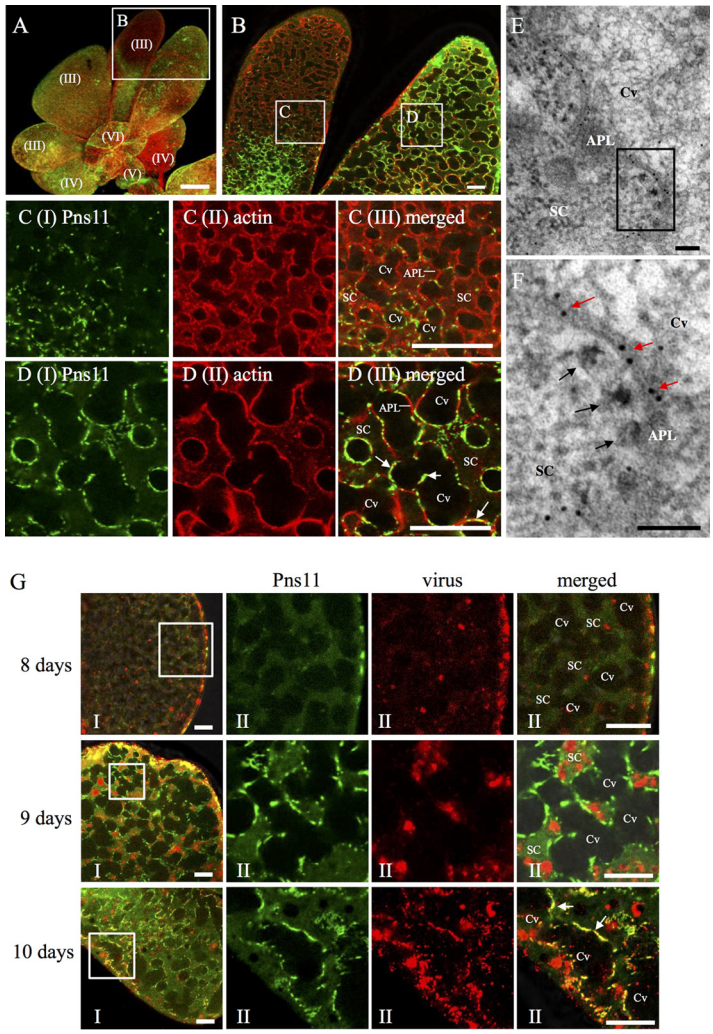

FIG 3 Immunofluorescence microscopy showing dissemination of RGDV into salivary cavities in the PSGs of *R. dorsalis*. (A to D) Pns11 of RGDV was closely associated with actin-based cavity plasmalemma in virus-infected PSG regions. PSGs were immunostained with Pns11-FITC (green) and actin dye phalloidin-rhodamine (red) and examined by immunofluorescence microscopy. Panel B shows an enlargement of the boxed area in panel A. Panels C and D show enlargements of the boxed areas labeled C and D, respectively, in panel B. Bar in panel A, 150 μm. Bars in panels B to D, 10 μm. (E, F) Immunoelectron micrographs showing the association of actin with the edges of invagination along the apical plasmalemma. PSGs were immunolabeled with actin-specific IgG as primary antibodies, followed by treatment with 10-nm gold particle-conjugated goat antibodies against mice IgG as secondary antibodies. Red arrows mark gold particles. Black arrows mark viral particles. Panel F shows an enlargement of the boxed area in panel E. Bars, 100 nm. (G) Distribution of RGDV and Pns11 in the secretory cells of PSGs. PSGs at 8, 9, and 10 days padp were dissected and immunostained with Pns11-FITC (green) and virus-rhodamine (red). Panels II show enlargements of the boxed areas in panels I. The arrows mark the association of Pns11 with cavity. Bars, 20 μm. APL, apical plasmalemma; Cv, cavity; SC, salivary cytoplasm.

associated with the cavity plasmalemma, while viruses still were accumulated in the cytoplasm of secretory cells (Fig. 3G). At 10 days padp, RGDV particles were accompanied by Pns11 filaments on the plasmalemma, and they were also observed to accumulate in the cavities (Fig. 3G). Together, our results suggested that the dissemination of RGDV particles into the PSG cavities may involve a Pns11-mediated exocytosis-like mechanism.

RGDV Pns11 formed filament-like inclusions and interacted with cytoplasmic actin of *R. dorsalis*. Pns11-specific IgG specifically recognized filamentous or tubular structures in insect vectors (Fig. 2). To determine how Pns11 of RGDV can assemble different structures, the location and morphology of Pns11 expressed in Sf9 cells were

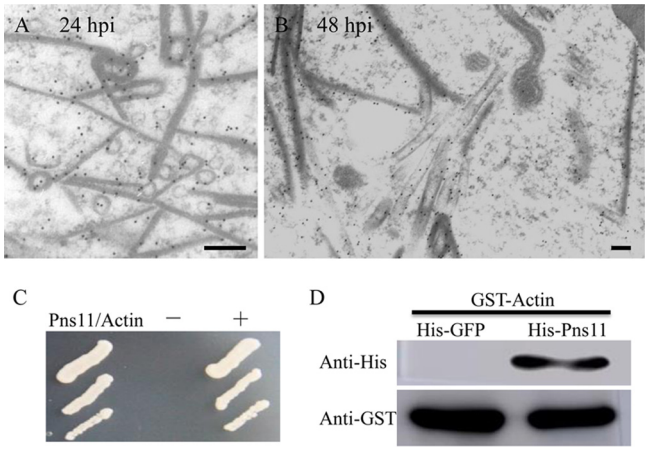

FIG 4 Interaction of Pns11 of RGDV with cytoplasmic actin of *R. dorsalis*. (A, B) Subcellular locations of Pns11 in recombinant baculovirus-infected Sf9 cells at 24 hpi (A) and 48 hpi (B). Sf9 cells were immunolabeled with Pns11-specific IgG as primary antibodies, followed by treatment with 15-nm gold particle-conjugated goat antibodies against rabbit IgG as secondary antibodies. Bars, 100 nm. (C) A yeast two-hybrid assay was used to detect the interaction of Pns11 and cytoplasmic actin of *R. dorsalis*. Transformants on an SD-Trp-Leu-His-Ade agar plate are shown. +, positive control, i.e., pBT3-STE and pOstl-Nubl; −, negative control, i.e., pBT3-STE and pPR3-N; Pns11/Actin, pBT3-STE-Pns11 and pPR3-N-actin. (D) A pulldown assay was used to analyze the interaction of Pns11 and cytoplasmic actin of *R. dorsalis*. Pns11 was fused with His to act as bait protein with GFP as a control. Cytoplasmic actin of *R. dorsalis* was fused with GST as a prey protein. Actin bound to His-fused Pns11 of RGDV but did not bind to His-fused GFP.

then observed via immunoelectron microscopy. We found that Pns11 of RGDV initially assembled the filamentous structures in the cytoplasm of Sf9 cells at 24 h postinoculation (hpi) (Fig. 4A). At 48 hpi, the tubulelike structures constructed by Pns11 could be clearly observed, as described previously (Fig. 4B). Thus, virus-associated filaments observed in the salivary glands of viruliferous *R. dorsalis* may be formed by Pns11 independent of other viral proteins, as we observed for the function of Pns11 in Sf9 cells. Our previous results have revealed that insect actin filaments can be recruited to enclose the tubules induced by two plant reoviruses, RDV and SRBSDV, via a direct interaction of actin and tubular proteins (8, 9). The association of Pns11 filaments of RGDV with actin-based cavity plasmalemma suggests a direct interaction of Pns11 with the cytoplasmic actin, the main component of cavity plasmalemma. The yeast two-hybrid assay demonstrated that Pns11 of RGDV specifically interacted with the cytoplasmic actin of *R. dorsalis* (Fig. 4C). A glutathione *S*-transferase (GST) pulldown assay confirmed that the GST-fused actin of *R. dorsalis* specifically bound to His-fused Pns11 of RGDV but did not bind to His-fused green fluorescent protein (GFP) (the negative bait control) (Fig. 4D). Thus, the association of Pns11 filaments with cavity plasmalemma was mediated by a specific interaction between Pns11 and cytoplasmic actin. Because RGDV particles have been ascertained to have the ability to attach to viral inclusions formed by Pns11 (19, 21), it appears that RGDV can hijack Pns11 filaments to perform an exocytosis-like process for viral release through actin-based apical plasmalemma into cavities of vector salivary glands.

Failure of Pns11 filament formation due to RNAi arrested the dissemination of RGDV into the cavity of vector salivary glands. We then examined the crucial role played by Pns11 of RGDV in viral release from vector salivary glands by RNA interference (RNAi) induced by microinjection of synthesized dsRNAs. The nymphs of *R. dorsalis* were fed on virus-infected rice plants. At 8 days after viral acquisition, RGDV had spread into the PSGs in about 65% of leafhoppers tested, as revealed by immunofluorescence microscopy (Fig. 3G). Such PSGs were suitable to test whether the failure of Pns11 filament formation due to RNAi inhibited viral dissemination into salivary cavities. Three days after microinjection of dsRNAs, immunofluorescence microscopy showed that RGDV had accompanied Pns11 filaments on the plasmalemma and invaded PSG

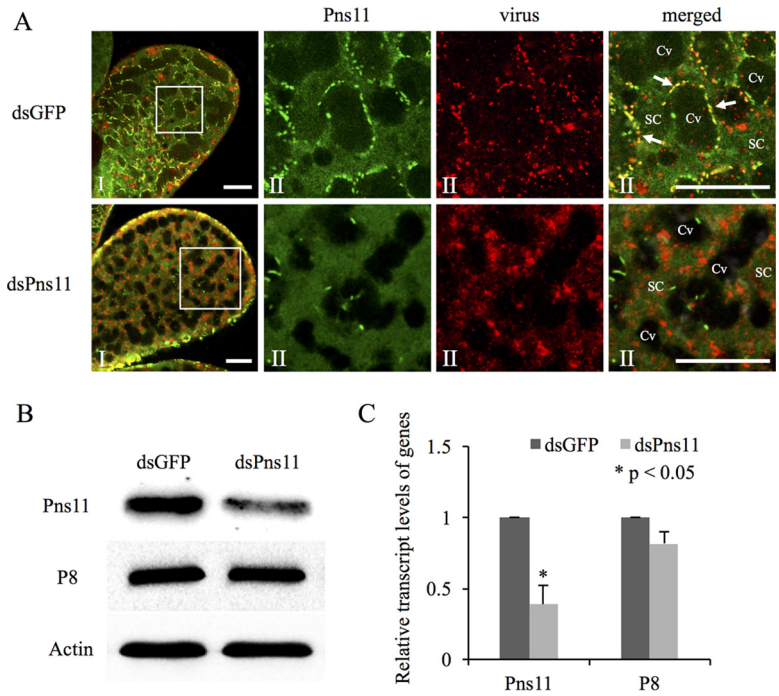

FIG 5 Microinjection of dsPns11 inhibited Pns11 filament formation and the subsequent transmission of RGDV by *R. dorsalis*. (A) Three days after microinjection with dsGFP or dsPns11, the PSGs of *R. dorsalis* were immunolabeled with Pns11-FITC (green) and virus-rhodamine (red) and then examined via confocal microscopy. Panels II show enlargements of the boxed areas in panels I. Cv, cavity; SC, salivary cytoplasm. Bars, 20 μm. All immunofluorescence figures are representative of at least three repetitions. (B) Detection of viral proteins Pns11 and P8 of RGDV in *R. dorsalis* by Western blotting assay with Pns11-specific or P8-specific IgGs. Insect actin was detected with actin-specific IgG as a control. (C) Detection of transcript levels for Pns11 or P8 genes in *R. dorsalis* by RT-qPCR assay, with means (±SD) from three independent experiments. *, $P < 0.05$.

cavities in about 70% of leafhoppers microinjected with dsGFP (Fig. 5A and Table 1). However, the microinjection with dsPns11 efficiently inhibited the formation of Pns11 filaments and strongly blocked viral accumulation along the plasmalemma and subsequent dissemination into PSG cavities (Fig. 5A and Table 1). The virus invaded PSG cavities in only about 31% of leafhoppers microinjected with dsPns11 (Fig. 5A and Table 1). The effects of dsPns11 treatment on the accumulation of major outer capsid protein P8 and Pns11 of RGDV in PSGs was further analyzed by Western blotting assays with Pns11- and P8-specific IgGs, respectively. As expected, dsPns11

TABLE 1 Treatment with dsPns11 via microinjection suppressed viral release into PSG cavities of *R. dorsalis* and suppressed viral transmission from insect vectors to rice plants[e]

Treatment[a]	Mean no. (± SE) of PSGs with viral antigens and Pns11 filaments in the cytoplasm or cavity (n = 50)[b]		Transmission rate (%) of RGDV from individual dsGFP- or dsPns11-treated *R. dorsalis* to rice plants[c]
	Cytoplasm (limited)	Cytoplasm and cavity (extensive)	
dsGFP	42.3 ± 1.8	35 ± 2.1	65.8 ± 3.8
dsPns11	40 ± 1.5	15.3 ± 0.9	32.4 ± 2.8
P value[d]	0.374	0.001	0.004

[a]Nymphs of *R. dorsalis* at 8 days padp were microinjected with 200 nl dsGFP or dsPns11 (0.5 g/liter), and a single rice plant was fed to individual dsGFP- or dsPns11-treated *R. dorsalis* for 2 days.
[b]Occurrence of RGDV antigens and Pns11 in PSGs of *R. dorsalis* was detected via immunofluorescence microscopy 3 days after microinjection.
[c]Transmission rate is the number of positive rice plants/total number of survival rice plants fed by dsRNAs-treated leafhoppers.
[d]P values were estimated by Tukey's honest significant difference (HSD) test (at P values of 0.05).
[e]Values are from three replicates.

treatment caused a significant reduction of Pns11 expression but did not significantly affect P8 accumulation in virus-infected vector PSGs (Fig. 5B). Furthermore, reverse transcription-quantitative PCR (RT-qPCR) assays confirmed that dsPns11 treatment resulted in a marked reduction of the transcript levels of Pns11 gene, but without a significant effect on the transcript levels of P8 gene (Fig. 5C), a finding consistent with its failure to effectively inhibit viral replication in the continuous cell line derived from *R. dorsalis* (21). Taken together, our results demonstrated that the failure of Pns11 filament formation efficiently prevented viral invasion into the cavities but did not significantly affect the normal replication and accumulation of RGDV in vector salivary glands.

To determine whether this failure of viral release into salivary cavities affected the transmission of RGDV via insect vectors, 30 individual leafhoppers microinjected with dsGFP or dsPns11 were fed on individual rice seedlings in individual tubes to test the transmission rates. As expected, the mean transmission rates of RGDV from individual dsGFP- or dsPns11-treated viruliferous *R. dorsalis* to rice plants were approximately 66% and 32%, respectively (Table 1). In summary, these data suggested that Pns11 of RGDV was essential for viral transmission by mediating viral dissemination via the apical plasmalemma into the cavities of vector salivary glands.

DISCUSSION

Here, we determined that a propagative virus, RGDV, can exploit virus-induced inclusions for efficient dissemination of virions through the last membrane barrier, the apical plasmalemma of salivary cavities of its insect vectors. Free virions of nonpropagative luteoviruses and propagative rhabdoviruses overcome this barrier via transcytosis or membrane budding (2, 6). However, the apical plasmalemma of salivary cavities in the leafhopper vector seems to lack the necessary cellular receptors for the attachments of free RGDV virions. We thus hypothesize that virus-induced inclusions may mediate viral dissemination from this membrane barrier. Virus-associated filaments constructed by the nonstructural protein Pns11 of RGDV specifically attached to the surface of cavity plasmalemma through a direct interaction of Pns11 and cytoplasmic actin, the main component of cavity plasmalemma (Fig. 1 to 4). Such attachment further induced an exocytosis-like process for viral release into the cavity, involving membrane curvature, the formation of invaginations, and the creation of vesicular compartments (Fig. 1). Morphologically, the release process of RGDV into the salivary cavity is different from the previously reported transcytosis exploited by nonpropagative luteovirus while passing through the apical plasmalemma of the salivary glands in its aphid vector (6, 12). Actually, if we regard the salivary cavity as one cell, then the exocytosis-like process for viral release into the cavity resembles the early stage of viral entry into insect vector cells via clathrin-mediated endocytosis (25). The Pns11-mediated exocytosis-like process is a newly described mechanism for viral particles passing through a cellular membrane.

Failure of Pns11 filament formation as a result of RNAi induced via synthesized dsPns11 inhibited the release of RGDV into the cavities but did not significantly affect viral accumulation in the cytoplasm of salivary gland cells (Fig. 5 and Table 1). Based on the discussions presented above, we propose that RGDV has developed a novel ability to hijack Pns11 filaments to perform an exocytosis-like process for viral particles passing through the apical plasmalemma into the cavities of vector salivary glands (Fig. 6). It is clear that the nonstructural protein Pns11 of RGDV can act as a viral determinant for transmission by insect vectors. Once inside the cavities, virions can move with the watery saliva into a duct that ultimately allows virus-laden saliva to excrete into the stylets and then be introduced into the phloem of host plants. Whether saliva components are necessary for viral infection in plant hosts is still unknown. For the first time, we show that a virus has the ability to exploit viral inclusions to overcome salivary gland release barrier of insect vectors.

Expression of Pns11 in Sf9 cells, nonhosts of RGDV, resulted in the formation of filament- or tubule-like structures (Fig. 4). Thus, Pns11 was the minimal viral factor

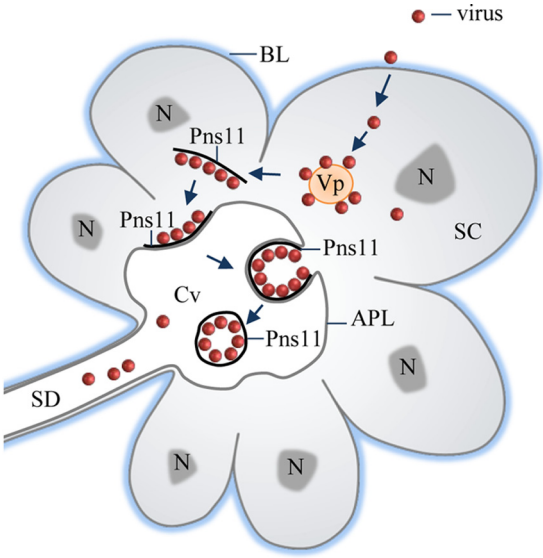

FIG 6 Proposed model for Pns11 filament-mediated dissemination of RGDV into the apical plasmalemma-lined cavities in the salivary glands of *R. dorsalis*. Viruses first enter the cytoplasm of secretory cells and then initiate multiplication processes for the assembly of progeny virions. Some virions are associated with virus-induced Pns11 filaments in the cytoplasm. These virus-associated filaments induce an exocytosis-like process to pass through the apical plasmalemma into the salivary cavity, facilitating viral release from secretory cells and finally into the salivary duct. Arrows indicate the process of viral release from salivary glands. APL, apical plasmalemma; BL, basal lamina; Cv, cavity; N, nucleus; SC, salivary cytoplasm; SD, salivary duct; Vp, viroplasm.

required for the formation of virus-induced filaments or tubules during RGDV infection of insect vectors. It appeared that the filaments were the intermediate structures to assemble the tubules. Our previous observation finds that virus-containing tubules constructed by the nonstructural protein Pns10 of RDV, the functional counterpart of Pns11 of RGDV, facilitate viral spread in the midgut of insect vectors (8, 17, 21). Similarly, we confirmed that virus-containing tubules induced by RGDV infection were also distributed along actin-based midgut microvilli or muscle fibers of viruliferous *R. dorsalis* (Fig. 2), suggesting that RGDV may exploit such tubules to spread in the vector midguts. Clearly, Pns11-induced inclusions (such as tubules or filaments) were the matrices for the attachment of free RGDV particles in insect vectors.

Interestingly, the filaments were specifically formed in the PSGs, whereas the tubules were specifically formed in the midguts (Fig. 2). We deduced that the filaments may confer a selective advantage for the release of RGDV into the cavity, because the filamentous matrix would provide a larger surface area for the attachment of cavity plasmalemma or viral particles, as shown in Fig. 1 and 3.

RGDV is transmitted by *R. dorsalis* with high efficiency (15, 26), suggesting that abundant virions must be efficiently released from vector PSGs. The apical plasmalemma of salivary cavities forms a loose network and provides large surface areas in the secretory cells (Fig. 2 and 3). Furthermore, virus-loaded Pns11 filaments are closely associated with the whole apical plasmalemmas in virus-infected regions (Fig. 2 and 3). These two factors can guarantee efficient transmission of abundant virions from salivary glands into plant hosts. As a propagative virus, RGDV must replicate and produce abundant progeny virions in the salivary gland cells to ensure efficient transmission, and a single cycle for viral multiplication in infected cells will take at least 24 h (7). Based on our current model for the release of RGDV from salivary glands, we suggest that the formation of adequate amounts of Pns11 filaments and the assembly of abundant progeny virions are prerequisites for high-efficiency transmission via vectors. In general, one typical characteristic for the transmission of rice reoviruses via insect vectors is intermittent (7, 26); however, the mechanism is still poorly understood. We deduce that the period for producing abundant Pns11 filaments or

progeny virions for transmission may be one of the reasons of intermittent transmission of RGDV by insect vectors.

All arboviruses and propagative plant viruses can replicate and induce viral inclusions in their respective insect vectors (1). Our current model could be extensively exploited by these propagative viruses to overcome salivary gland release barriers in respective insect vectors, opening new perspectives for viral control. However, few molecular determinants are clearly known to be active during viral release from vector salivary glands. Previously, innate immune responses, apoptosis, or autophagy has been reported to be induced by viral infection of insect salivary glands (27–30). How viruses exploit these cellular structures or pathways to overcome salivary gland barriers should be investigated in the future.

MATERIALS AND METHODS

Insects, virus, and antibodies. RGDV samples, collected from rice fields from Guangdong Province, China, were maintained on rice plants via transmission by *R. dorsalis*, as previously described (16). Polyclonal antibodies against intact viral particles, major outer capsid protein P8, and nonstructural proteins Pns4, Pns7, Pns9, Pns10, Pns11, and Pns12 of RGDV were prepared as previously described (15, 19, 21). IgGs were purified from polyclonal antibodies and then conjugated directly to fluorescein isothiocyanate (FITC) or rhodamine (Invitrogen) according to the manufacturer's instructions.

Immunofluorescence staining of leafhopper salivary glands after viral acquisition. Second-instar nymphs of *R. dorsalis* were fed on diseased rice plants for 1 day and then transferred to healthy rice seedlings. At different days padp, salivary glands from 50 individuals of *R. dorsalis* were dissected, fixed, and immunolabeled with virus-specific IgG conjugated to FITC (virus-FITC) and actin dye phalloidin-rhodamine (Invitrogen), or with Pns11-specific IgG conjugated to FITC (Pns11-FITC) and actin dye phalloidin-rhodamine (Invitrogen), or with Pns11-FITC and virus-specific IgG conjugated to rhodamine (virus-rhodamine), as previously described (9). The samples were then examined with a Leica TCS SP5II confocal microscope. The salivary glands dissected from *R. dorsalis* insects that were fed on healthy rice plants were treated in exactly the same way and served as controls.

Electron microscopy. Sf9 cells infected with recombinant baculovirus vector containing Pns11 of RGDV have been previously described (21). The midguts and salivary glands dissected from viruliferous *R. dorsalis* or Sf9 cells were fixed, dehydrated, and embedded, and ultrathin sections were cut as previously described (9). For immunoelectron microscopy, sections were immunolabeled with the Pns11- or actin-specific IgGs as primary antibodies, followed by treatment with goat anti-rabbit IgG conjugated with 10- or 15-nm-diameter gold particles as secondary antibodies (Abcam), as previously described (21).

Yeast two-hybrid assay. A yeast two-hybrid assay was performed using a DUALmembrane starter kit (DUALsystems Biotech) according to the manufacturer's instructions. The Pns11 gene of RGDV was cloned into the bait vector PBT-STE, and the cytoplasmic actin gene of *R. dorsalis* was cloned into the prey vector pPR3-N. The recombinant plasmids PBT-STE-Pns11 and pPR3-N-actin as well as PBT-STE-Pns11 and pPR3-N were cotransformed with *Saccharomyces cerevisiae* (strain NMY51). Plasmids pTSU2-APP and pNubG-Fe65 (positive control) or plasmid pPR3-N (negative control) was cotransformed into NMY51. All transformants were grown on synthetic dropout (SD)-Trp-Leu-His-Ade agar plates for 3 to 4 days at 30°C.

Pulldown assay. The Pns11 gene of RGDV and the GFP gene were cloned into pBT30a for His tag fusion. The actin gene of *R. doralis* was cloned into PGEX-3 for fusion with GST. All recombinant proteins were expressed in *Escherichia coli* (strain BL21). GST-actin was incubated with glutathione-Sepharose beads (Amersham) for 4 h at 4°C. His-Pns11 or His-GFP was added to the beads, and the mixture was incubated for 4 h at 4°C. The beads were collected and washed with wash buffer (300 mM NaCl, 10 mM Na_2HPO_3, 2.7 mM KCl, and 1.7 M KH_2PO_4). Immunoprecipitated proteins were detected by Western blotting assay with His-tagged and GST-tagged antibodies (Sigma) separately.

Effects of synthesized dsRNAs on viral accumulation and transmission by *R. dorsalis*. A T7 RiboMAX Express RNA interference (RNAi) system kit (Promega) was utilized for *in vitro* synthesis of dsRNAs for Pns11 or GFP genes (dsPns11 or dsGFP) according to the manufacturer's instructions. The 400-s instar nymphs of *R. dorsalis* were fed on RGDV-infected rice plants for 1 day and then kept on healthy rice seedlings for 7 days. Individual nymphs were then microinjected with 200 nl dsGFP or dsPns11 (0.5 g/liter) and kept on healthy rice seedlings, as previously described (15). Three days after microinjection, the salivary glands from 50 leafhoppers were dissected, fixed, immunolabeled with Pns11-FITC and virus-rhodamine, and then processed for immunofluorescence microscopy. The PSGs with viral distribution in the cytoplasm or cavity in each group were counted, and the mean value was calculated based on three replicates. Furthermore, the total proteins were extracted from dissected salivary glands from dsRNA-treated leafhoppers. The accumulation of Pns11 and P8 of RGDV were analyzed by Western blotting assay with Pns11- and P8-specific IgGs, respectively. To measure the effects of dsRNAs on the transcript levels of Pns11 and P8 genes, the total RNAs were extracted from dissected salivary glands from dsRNA-treated leafhoppers. Relative RT-qPCR assays were performed to analyze the relative levels of gene expression by the $2^{-\Delta\Delta CT}$ method (where C_T is threshold cycle). A pool of 50 leafhoppers were used for RNA extraction and RT-qPCR assay, which was repeated three times.

To determine whether the microinjection of dsRNAs affected the transmission of RGDV by insect vectors, individual viruliferous leafhoppers microinjected with dsRNAs were exposed to a single healthy

rice seedling in individual tubes for a 2-day inoculation access feeding and then transferred to a new healthy seedling. One insect inoculated six rice seedlings sequentially, and the rice plants were tested for visible symptoms. Total RNA was extracted from inoculated seedlings to determine the presence of transcript for the RGDV P8 gene to calculate transmission rates. For each treatment, a group of 30 leafhoppers was used for viral transmission test. The transmission rates of each group were calculated according to the number of virus-infected rice plants/total number of survival rice plants fed by dsRNAs-treated leafhoppers, and the mean value was calculated based on three replicates.

Statistical analyses. All data were analyzed for statistical significance with SPSS, version 17.0. Multiple comparisons of the means were conducted based on Tukey's honestly significant difference (HSD) test using a one-way analysis of variance (ANOVA).

ACKNOWLEDGMENTS

We thank Toshihiro Omura for providing polyclonal antiserum against intact viral particles.

The National Science Foundation for Outstanding Youth provided funding to Taiyun Wei under grant number 31325023. The National Basic Research Program of China provided funding to Taiyun Wei under grant number 2014CB138400. The National Natural Science Foundation of China provided funding to Qianzhuo Mao under grant number 31401712. The Natural Science Foundation of Fujian Province provided funding to Qianzhuo Mao under grant number 2015J01087.

REFERENCES

1. Hogenhout SA, Ammar ED, Whitfield AE, Redinbaugh MG. 2008. Insect vector interactions with persistently transmitted viruses. Annu Rev Phytopathol 46:327–359. https://doi.org/10.1146/annurev.phyto.022508.092135.
2. Ammar ED, Tsai CW, Whitfield AE, Redinbaugh MG, Hogenhout SA. 2009. Cellular and molecular aspects of Rhabdovirus interactions with insect and plant hosts. Annu Rev Entomol 54:447–468. https://doi.org/10.1146/annurev.ento.54.110807.090454.
3. Blanc S, Drucker M, Uzest M. 2014. Localizing viruses in their insect vectors. Annu Rev Phytopathol 52:403–425. https://doi.org/10.1146/annurev-phyto-102313-045920.
4. Whitfield AE, Falk BW, Rotenberg D. 2015. Insect vector-mediated transmission of plant viruses. Virology 479:278–289. https://doi.org/10.1016/j.virol.2015.03.026.
5. Gray S, Gildow F. 2003. Luteovirus-aphid interactions. Annu Rev Phytopathol 41:539–566. https://doi.org/10.1146/annurev.phyto.41.012203.105815.
6. Brault V, Herrbach E, Reinbold C. 2006. Electron microscopy studies on luteovirid transmission by aphids. Micron 38:302–312. https://doi.org/10.1016/j.micron.2006.04.005.
7. Wei T, Li Y. 2016. Rice reoviruses in insect vectors. Annu Rev Phytopathol 54:99–120. https://doi.org/10.1146/annurev-phyto-080615-095900.
8. Chen Q, Chen H, Mao Q, Liu Q, Shimizu T, Uehara-Ichiki T, Wu Z, Xie L, Omura T, Wei T. 2012. Tubular structure induced by a plant virus facilitates viral spread in its vector insect. PLoS Pathog 8:e1003032. https://doi.org/10.1371/journal.ppat.1003032.
9. Jia D, Mao Q, Chen H, Wang A, Liu Y, Wang H, Xie L, Wei T. 2014. Virus-induced tubule: a vehicle for rapid spread of virions through basal lamina from midgut epithelium in the insect vector. J Virol 88:10488–10500. https://doi.org/10.1128/JVI.01261-14.
10. Wu W, Zheng L, Chen H, Jia D, Li F, Wei T. 2014. Nonstructural protein NS4 of rice stripe virus plays a critical role in viral spread in the body of vector insects. PLoS One 9:e88636. https://doi.org/10.1371/journal.pone.0088636.
11. Montero-Astúa M, Ullman DE, Whitfield AE. 2016. Salivary gland morphology, tissue tropism and the progression of tospovirus infection in *Frankliniella occidentalis*. Virology 493:39–51. https://doi.org/10.1016/j.virol.2016.03.003.
12. Gildow FE. 1982. Coated vesicle transport of luteoviruses through salivary glands of *Myzus persicae*. Phytopathology 72:1289–1296. https://doi.org/10.1094/Phyto-72-1289.
13. Wei J, Zhao J, Zhang T, Li F, Ghanim M, Zhou X, Ye G, Liu S, Wang X. 2014. Specific cells in the primary salivary glands of the whitefly *Bemisia tabaci* control retention and transmission of Begomoviruses. J Virol 88:13460–13468. https://doi.org/10.1128/JVI.02179-14.
14. Omura T, Inoue H, Morinaka T, Saito Y, Chettanachit D, Putta M, Parejarearn A, Disthaporn S. 1980. Rice gall dwarf, a new virus disease. Plant Dis 64:795–797. https://doi.org/10.1094/PD-64-795.
15. Zheng L, Chen H, Liu H, Xie L, Wei T. 2014. Assembly of viroplasms by viral nonstructural protein Pns9 is essential for persistent infection of Rice gall dwarf virus in its insect vector. Virus Res 196:162–169. https://doi.org/10.1016/j.virusres.2014.11.025.
16. Miyazaki N, Hagiwara K, Naitow H, Higashi T, Cheng R, Tsukihara T, Nakagawa A, Omura T. 2005. Transcapsidation and the conserved interactions of two major structural proteins of a pair of phytoreoviruses confirm the mechanism of assembly of the outer capsid layer. J Mol Biol 345:229–237. https://doi.org/10.1016/j.jmb.2004.10.044.
17. Moriyasu Y, Maruyama-Funatsuki W, Kikuchi A, Ichimi K, Zhong B, Yan J, Zhu Y, Suga H, Watanabe Y, Ichiki-Uehara T, Shimizu T, Hagiwara K, Kamiunten H, Akutsu K, Omura T. 2007. Molecular analysis of the genome segments S1, S4, S6, S7 and S12 of a Rice gall dwarf virus isolate from Thailand; completion of the genomic sequence. Arch Virol 152:1315–1322. https://doi.org/10.1007/s00705-007-0948-7.
18. Zhang H, Xin X, Yang J, Chen J, Wang J, Adams M. 2008. Completion of the genome sequence of Rice gall dwarf virus from Guangxi, China. Arch Virol 153:1737–1741. https://doi.org/10.1007/s00705-008-0167-x.
19. Wei T, Uehara-Ichiki T, Miyazaki N, Hibino H, Iwasaki K, Omura T. 2009. Association of Rice gall dwarf virus with microtubules is necessary for viral release from cultured insect vector cells. J Virol 83:10830–10835. https://doi.org/10.1128/JVI.01067-09.
20. Akita F, Miyazaki N, Hibino H, Shimizu T, Higashiura A, Uehara-Ichiki T, Sasaya T, Tsukihara T, Nakagawa A, Iwasaki K, Omura T. 2011. Viroplasm matrix protein Pns9 from Rice gall dwarf virus forms an octameric cylindrical structure. J Gen Virol 92:2214–2221. https://doi.org/10.1099/vir.0.032524-0.
21. Chen H, Zheng L, Jia D, Zhang P, Chen Q, Liu Q, Wei T. 2013. Rice gall dwarf virus exploits tubules to facilitate viral spread among cultured insect vector cells derived from leafhopper *Recilia dorsalis*. Front Microbiol 4:206. https://doi.org/10.3389/fmicb.2013.00206.
22. Sogawa K. 1971. Studies on the salivary glands of rice plant leafhoppers. Jpn J Appl Entomol Zool 15:132–138. https://doi.org/10.1303/jjaez.15.132.
23. Wei T, Miyazaki N, Uehara-Ichiki T, Hibino H, Shimizu T, Netsu O, Kikuchi A, Sasaya T, Iwasaki K, Omura T. 2011. Three-dimensional analysis of the association of viral particles with mitochondria during the replication of Rice gall dwarf virus. J Mol Biol 15:436–446. https://doi.org/10.1016/j.jmb.2011.05.017.
24. Lan H, Wang H, Chen Q, Chen H, Jia D, Mao Q, Wei T. 2016. Small interfering RNA pathway modulates persistent infection of a plant virus in its insect vector. Sci Rep 6:20699. https://doi.org/10.1038/srep20699.
25. Wei T, Chen H, Ichiki-Uehara T, Hibino H, Omura T. 2007. Entry of rice dwarf virus into cultured cells of its insect vector involves clathrin-mediated endocytosis. J Virol 81:7811–7815. https://doi.org/10.1128/JVI.00050-07.

26. Hibino H. 1996. Biology and epidemiology of rice viruses. Annu Rev Phytopathol 34:249–274. https://doi.org/10.1146/annurev.phyto.34.1.249.
27. Kelly EM, Moon DC, Bowers DF. 2012. Apoptosis in mosquito salivary glands: Sindbis virus-associated and tissue homeostasis. J Gen Virol 93:2419–2424. https://doi.org/10.1099/vir.0.042846-0.
28. Wang H, Gort T, Boyle DL, Clem RJ. 2012. Effects of manipulating apoptosis on Sindbis virus infection of *Aedes aegypti* mosquitoes. J Virol 86:6546–6554. https://doi.org/10.1128/JVI.00125-12.
29. Huang H, Bao Y, Lao S, Huang X, Ye Y, Wu J, Xu H, Zhou X, Zhang C. 2015. Rice ragged stunt virus-induced apoptosis affects virus transmission from its insect vector, the brown planthopper to the rice plant. Sci Rep 5:11413. https://doi.org/10.1038/srep11413.
30. Zhao W, Lu L, Yang P, Cui N, Kang L, Cui F. 2016. Organ-specific transcriptome response of the small brown planthopper toward rice stripe virus. Insect Biochem Mol Biol 70:60–72. https://doi.org/10.1016/j.ibmb.2015.11.009.